IMPACT STRENGTH AND RESPONSE BEHAVIOR OF CFRP GUARDER BELT FOR SIDE COLLISION OF AUTOMOBILES

AOKI Y.*, BEN G.**, KIM H. S.*
*College of Science & Technology, Nihon University
**College of Industrial Technology, Nihon University
7-24-1 Narashino-dai, Funabashi, Chiba 274-8501 JAPAN
aoki.yoshio@nihon-u.ac.jp

SUMMARY

In this paper, the CFRP guarder belt equipped in the automotive door is developed and examined by an experiment and a numerical analysis for replacing the conventional steel door guarder beam. As the experimental relation of impact load to displacement for CFRP guarder belt agreed well with that of numerical result, the numerical method developed here is quite useful for estimating impact behaviours of CFRP guarder belt.

Keywords: Impact behaviour, CFRP, Absorbed energy, Automobile, Collision safety

INTRODUCTION

It is well known that CO2 emissions, which are one of the greenhouse gases emitted from passenger vehicles such as automobile, are major cause of global warming. In the automobile industry, to reduce CO2 emissions, it is well known that the most effective method is to produce the fuel efficient automobile. To increase the fuel efficiency of the automobile, the most effective approach is to reduce the automobile weight by using lightweight material such as composite materials. Carbon fiber reinforced plastics (CFRP) have been widely used in aerospace, industrial goods and other application fields because of their high specific strength and high specific modulus compared with metal. This means that the CFRP contributes to lighten automobiles greatly. Otherwise, the safety of automobiles is also very important and the collision safety of the automobile has been evaluated by full flap frontal crash, offset frontal crash and side impact tests. In the frontal crash test, it is possible to absorb the energy by largely deforming the front part and the rear. With an increasing an interest in the lightening of the automobile and in the securing the safety of passengers, many researches for them have been performed [1-9]. However, in the side impact test, it is hard to absorb the energy similarly, because of being very narrow for the survival space of passengers. In the inside of the door, a reinforcement member as shown in Figure 1, namely door guarder beam made of steel has been installed to absorb impact energy and its deformation is limited to about 150mm.

In this study, the CFRP door guarder belt is developed for the purpose of designing impact energy absorption members under side collision as shown in Figure 2. A drop weight impact tests are carried out to investigate impact response behaviours and impact energy absorption characteristics of the CFRP door guarder belt. Also, a finite element

(FE) model was developed by using the ANSYS to simulate the impact response behaviour and the absorbed energy of the CFRP door guarder belt under impact loading.

Figure 1 Conventional door guarder beam

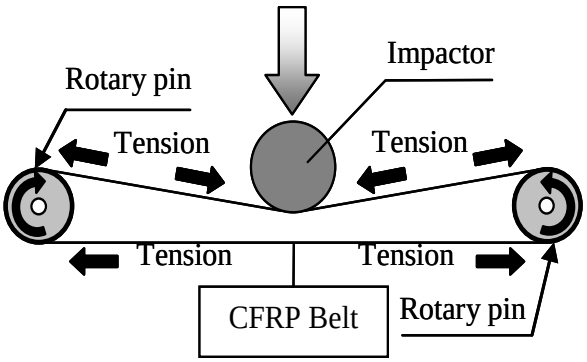

Figure 2 Energy absorption mechanism of CFRP guarder belt

EXPERIMENT

Specimen fabrication

Figure 2 shows the schematic diagram of the impact energy absorption by the CFRP guarder belt. The impact energy is effectively absorbed by installing the CFRP belt between two free fulcrums for the rotation and changing the vertical impact load of the falling weight to the tensile load. In order to prevent fracture in the support edge of specimen due to the stress concentration, a belt-shaped specimen was adopted. Thin CFRP belt specimens were manufactured from unidirectional prepregs (T800H/Epoxy) by using the sheet winding method and its thickness, width and length were 0.23mm, 50mm and 1642mm, respectively. Figure 3 shows an actual CFRP guarder belt.

Tower drop weight impact test

In order to evaluate the capacity of crash energy absorption and to show the micro and macro fracture behavior of the CFRP guarder belt, the large size of drop tower facility for the impact test was designed as shown in Figure 3. The CFRP guarder belt was received the impact load generated by a free drop weight of 100kg from 12m height. Therefore, the impact speed was approximately 55km/h just before the impact. The shape of impactor was a half cylinder having 100mm radius and 200mm width. The

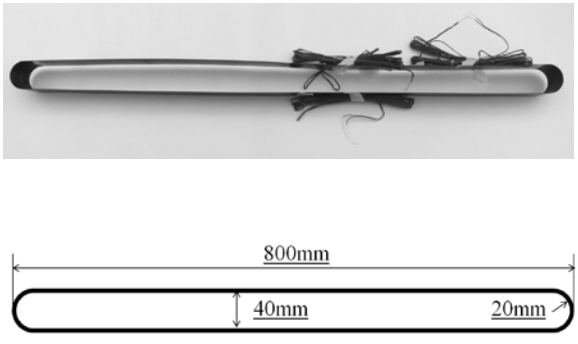

(a) CFRP guarder belt specimen

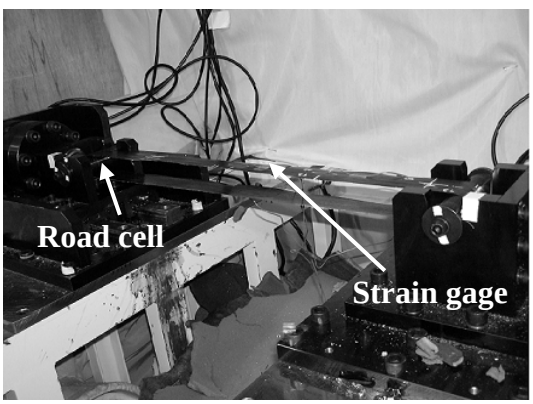

(b) mounted specimen

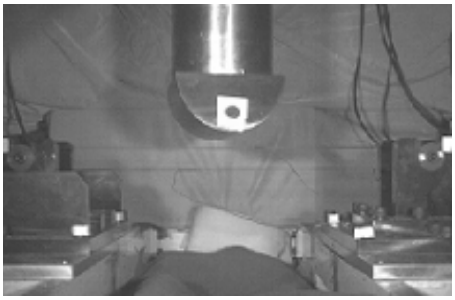

(c) Impactor

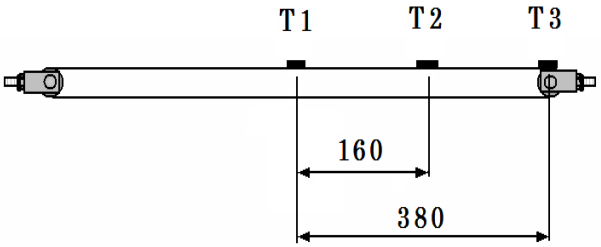

(d) measured location of the longitudinal strain

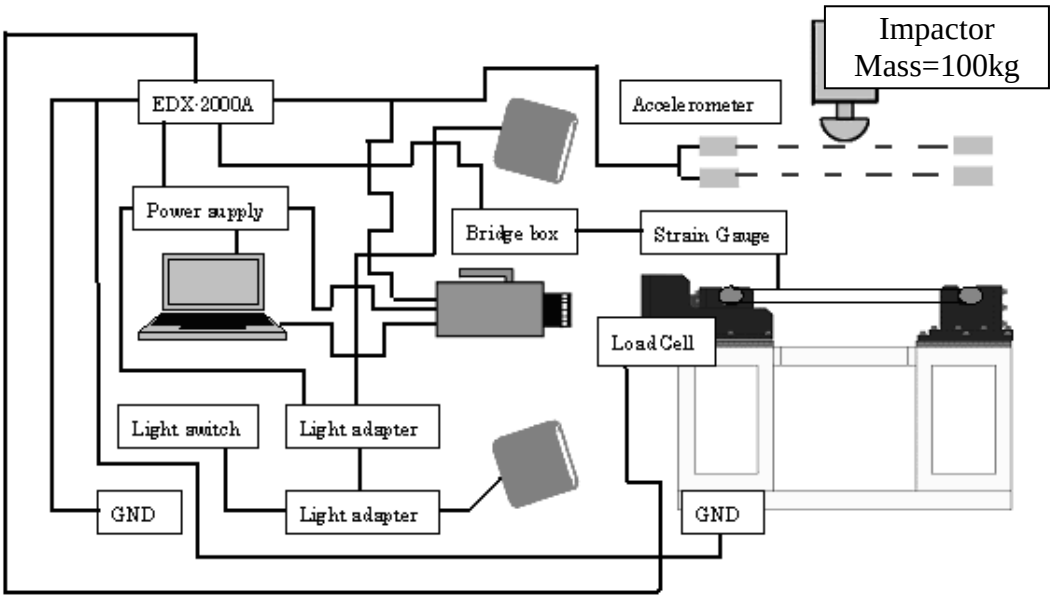

Figure 3 CFRP guarder belt specimen and Tower drop impact test setup

impact load of the specimen was measured by a load cell installed behind the rotary pin. In order to investigate the fracture mechanism of the CFRP guarder belt, a high- speed camera was chosen. And the dynamic strain of the specimen from collision to fracture was measured by a strain gauge. The strain gauge stuck on three places at the center of the specimen as a collision point (T1), near the rotary pin (T3) and middle point of both (T2) as shown in Figure 3. The CFRP guarder belt specimen supported both ends in the rotary pin of a diameter of 40mm.

Figure 4 shows the measured horizontal load and the longitudinal strain of the center of the specimen variation after impact. The horizontal impact load of CFRP belt specimen increase nonlinearly, and the impact load reached to the maximum and then instantly dropped to almost zero as shown in the left side of Figure 4. Within the time of 5.0~5.4msec, the impact load recovered to 38~40kN and become to zero at the displacement of about 85mm. The longitudinal strain of the specimen at the impact location also increases nonlinearly from a moment of impact, and becomes the maximum value just before fracture of the CFRP belt specimen.

Figure 5 shows the observed fracture modes and the fracture location of CFRP guarder belt specimen. In the experiment, the observed fracture mode was fiber breakage in the entire width of CFRP belt specimen due to the tensile load acted on the whole the

specimen. And almost specimen fractured at the location of T3, that is larger tensile stress occurred around the rotary pin is supposed.

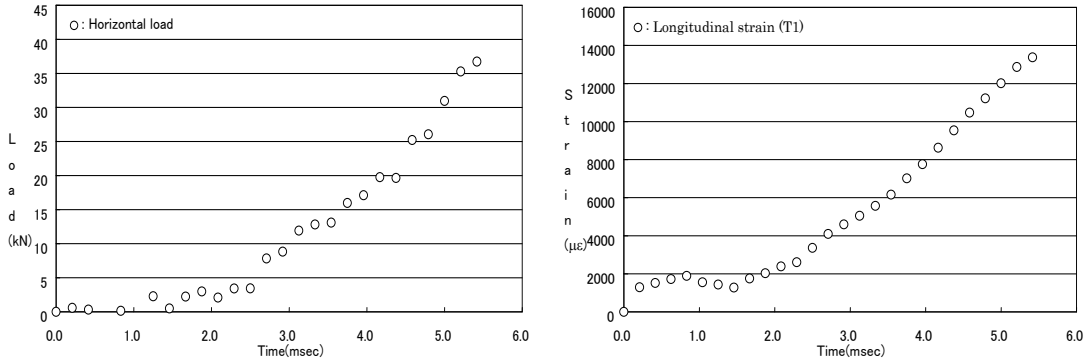

Figure 4 Horizontal load and Strain of the center of the specimen variation after impact

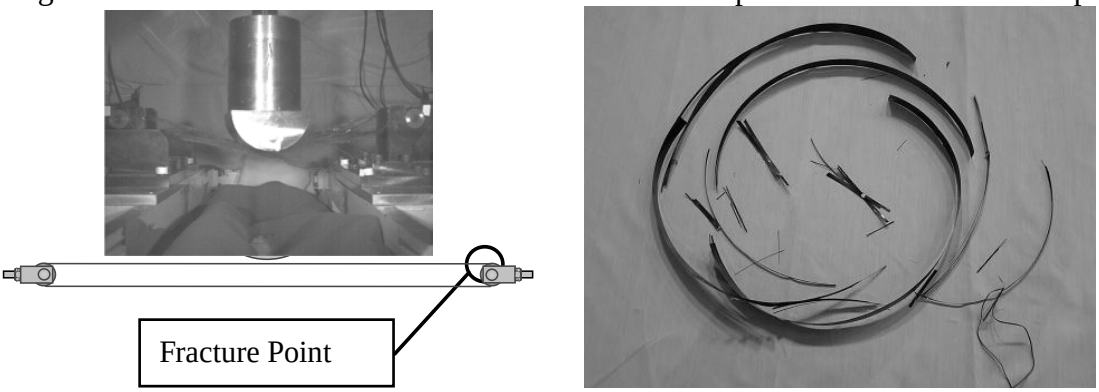

Figure 5 Fracture mode of CFRP in the impact test for the CFRP guarder belt

Figure 6 shows the comparison of experimental load-displacement curve between the vertical impact and the impact with offset angle of 15°. The horizontal load of the impact with offset angle of 15° increases nonlinearly until the displacement of 80mm, and it's almost same tendency for the vertical impact case. The maximum impact load for offset impact case is 24% smaller than the vertical impact case.

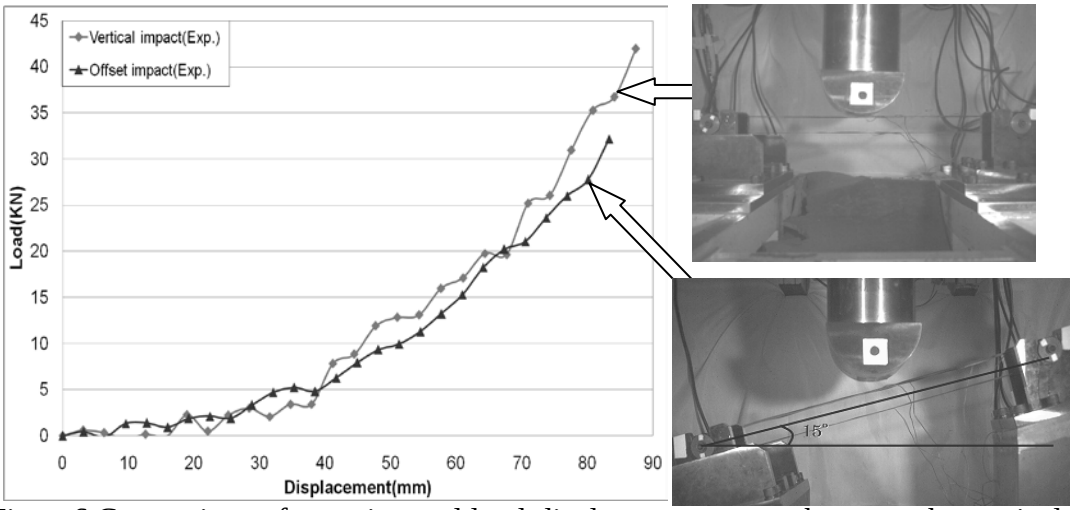

Figure6 Comparison of experimental load-displacement curves between the vertical impact and the impact with offset angle of 15°

NUMERICAL ANALYSIS

To simulate the impact response behavior and absorbed energy of the CFRP guarder belt under impact loading, a finite element model was developed by using the commercial FEM solver (ANSYS). In this FE analysis, the laminated shell element (SHELL_63) and the solid element (SOLID_45) were used in the CFRP guarder belts and the impactor and rotary pins, respectively. Details of the finite element model are shown in Figure 7. The contact element between the impactor and the upper surface of CFRP guarder belt and between the rotary pins and the inner surface of the belt was Contact element 173 with the Target element 170 of the friction coefficients of 0.25. And, we adopted 1/2 models with a symmetric condition to reduce a calculation time. Table 1 shows the material properties of CFRP guarder belt used for the analysis.

Prediction of the Fracture time of CFRP guarder belt

Next, the fracture time of the CFRP guarder belt was predicted from the results of the numerical analysis by using the fracture criterion of composites. In case of the unidirectional reinforced CFRP, the material property in the transverse direction is same as that of thickness direction, therefore Tsai-Hill fracture criterion was used in this analysis.

$$\left(\frac{\sigma_L}{F_L}\right)^2 - \frac{\sigma_L \sigma_T}{F_L^2} + \left(\frac{\sigma_T}{F_T}\right)^2 + \left(\frac{\tau_{LT}}{F_{LT}}\right)^2 = 1 \qquad (1)$$

Where F_L, F_T and F_{LT} are the strength of the CFRP belt along the fiber direction, that of the transverse direction and that of the in-plane shear, respectively. The F_L being much bigger than the stress of the transverse direction σ_T for thin CFRP belt specimen, so that equation (1) can be rewritten as below

$$\left(\frac{\sigma_L}{F_L}\right)^2 + \left(\frac{\sigma_T}{F_T}\right)^2 + \left(\frac{\tau_{LT}}{F_{LT}}\right)^2 = 1 \qquad (2)$$

Substituting the occurred stress and the strength in fiber direction σ_L, those of transverse σ_T and those of membrane shear τ_{LT} in the equation 2, it can be consider the fracture of CFRP belt specimen when the value of the left-hand side become 1.

Calculation of the absorbed energy for CFRP guarder belt

The absorbed energy of CFRP guarder belt can be calculated by an area of the curve of an impact load P and a displacement of the impact location of the specimen δ until its fracture as

$$E(\delta) = \int P(\delta) d\delta \qquad (3)$$

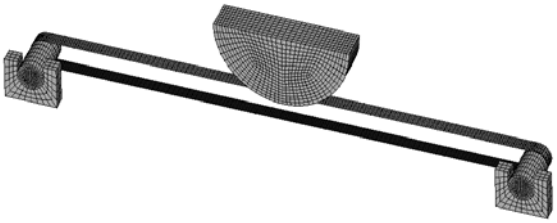

	CFRP Belt	Impactor, Coner Pin
Structual Element	Elastic Shell	3 - D Structural Solid
Contact Element	3 - D Target Segment	
	3 - D Surface - to Surface Contact	

Figure 7 Details of the finite element model

Table 1 Material properties of CFRP guarder belt

	CFRP Belt	Impactor, Coner Pin
E_x[GPa]	130	206
E_y[GPa]	8	-
E_z[GPa]	8	-
G_{xy}[GPa]	4	80
G_{yz}[GPa]	4	-
F_x[GPa]	2.45	-
F_y[GPa]	0.07	-
Fxy[GPa]	0.098	-
ν	0.34	0.3
Density[kg/m^3]	1600	8000

RESULTS AND DISCUSSIONS

Figure 8 shows the experimental and the numerical relation of impact load to displacement of the CFRP guarder belt for vertical impact. The experimental and numerical impact load increase with increasing the displacement of CFRP belt specimen nonlinearly, then, they become the maximum value just before fracture. The experimental and the numerical relation of impact load to displacement for CFRP guarder belt agreed well generally.

Next, Table 2 shows the predicted fracture time was calculated by equation (2), the location of fracture in the specimen and the absorbed energy obtained by FE analysis are compared with the experimental ones. The fracture time and the location of fracture are almost exactly predicted and the numerical absorbed energy is also close to the experimental ones. The specific absorbed energy divided by the individual weights of the CFRP guarder belt was compared with the conventional steel impact beam shown in Table 3. The conventional impact beam consists of steel pipe and has diameter of 35mm, thickness of 2mm and length of 945mm. Though experimental energy absorption of CFRP guarder belt is smaller than it of the conventional impact beam, the specific energy absorption of the CFRP belt is 30 times bigger than it of the impact beam. Therefore the energy absorption of CFRP belt bigger than the impact beam is possible if the width and thickness of the CFRP belt is increased.

The experimental strain variations at three locations in the specimen compare with the numerical ones as shown in Figure 9. The strain of each locations increase with time transit nonlinearly. The measured maximum impact strain at each location is almost same, though the numerical strain variation at the location of T3 is larger than experimental ones. This is because the numerical result wasn't considered a little looseness between the CFRP guarder belt and the rotary pin. Both results of the strain variations at the locations of T1 and T2 agreed well.

From the comparison of both results, the numerical method developed here is quite useful for estimating impact behavior of the CFRP guarder belt.

In the case of side collision, there is the collision from diagonal direction actually. Therefore, the impact response behavior for the side collision with offset angle of CFRP guarder belt was examined. The experiment of the side collision with offset angle was performed to incline the supported base of the specimen so that the impactor hit the specimen diagonally as shown in Figure 10. The drop weight impact test with offset angle of 15°was carried out in this experiment, then the difference in impact response behavior of the side collision was examined.

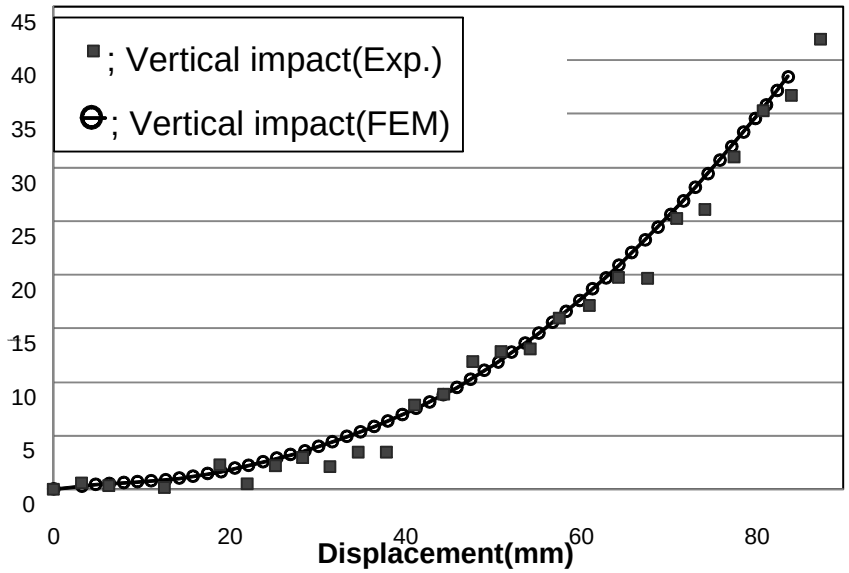

Figure 8 Comparison of experimental and predicted load-displacement curve of CFRP guarder belt for vertical impact

Table 2 Fracture time and absorbed energy of CFRP guarder belt for vertical impact

	Experiment	FEM
Fracture time (msec)	5.63	5.72
Location of the fracture	T3	T3
Absorbed energy (J)	1118	1010

Table 3 Comparison of Absorbed energy for CFRP guarder belt and steel impact beam

	Absorbed energy (J)	Specific absorbed energy (kJ/kg)
CFRP guarder belt	1118	37.14
Steel impact beam	1900	1.243

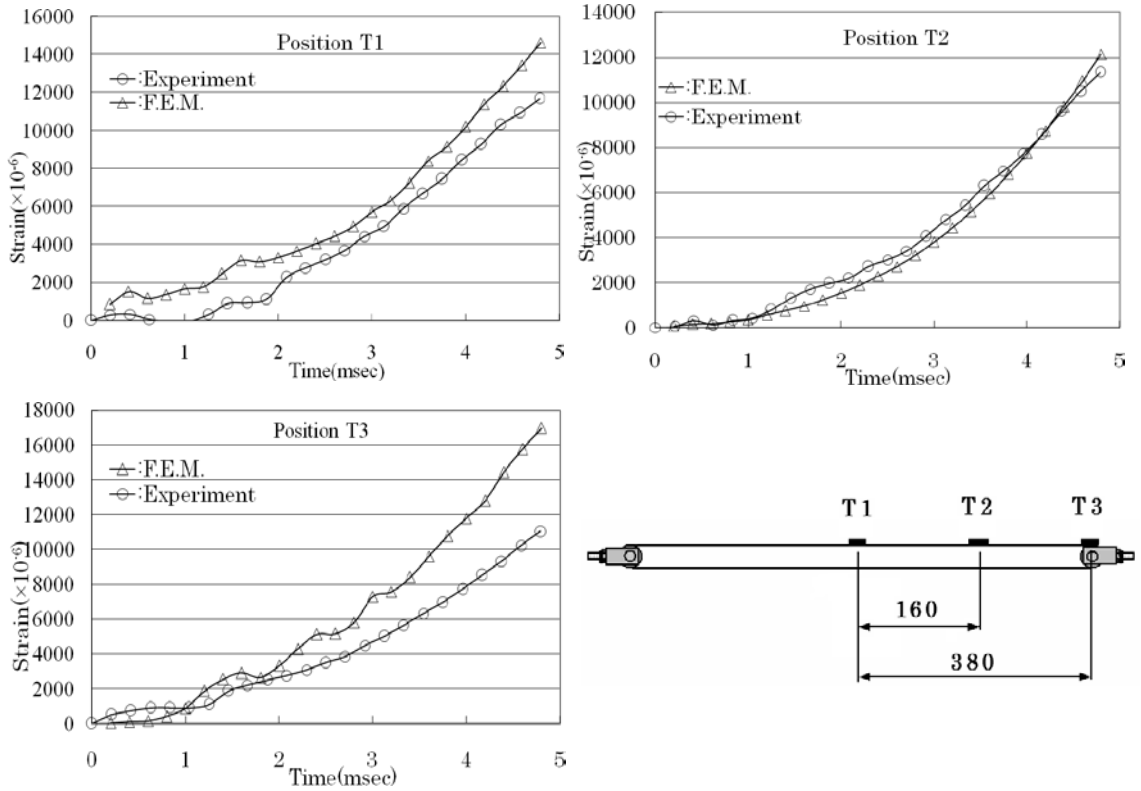

Figure 9 Comparisons of experimental and predicted the strain variation of CFRP guarder belt for vertical impact

Figure 11 shows the experimental and the numerical relation of impact load to displacement of the CFRP guarder belt for impact with offset angle of 15°. Though the maximum impact load by numerical result is slightly larger than experimental ones, both relation of impact load to displacement for CFRP guarder belt agreed well generally.

Table 4 shows the predicted fracture time, the location of fracture in the specimen and the absorbed energy obtained by FE analysis are compared with the experimental ones

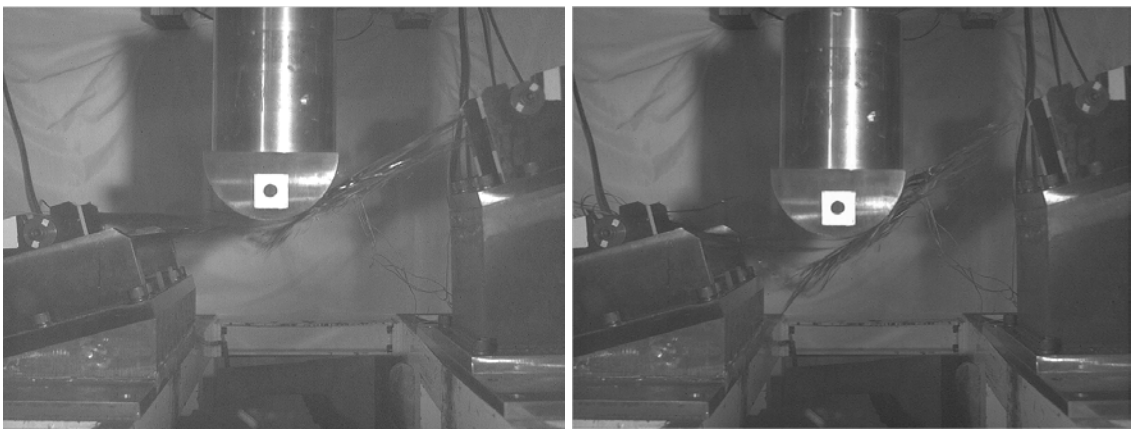

Figure 10 The drop weight impact test with offset angle of 15°

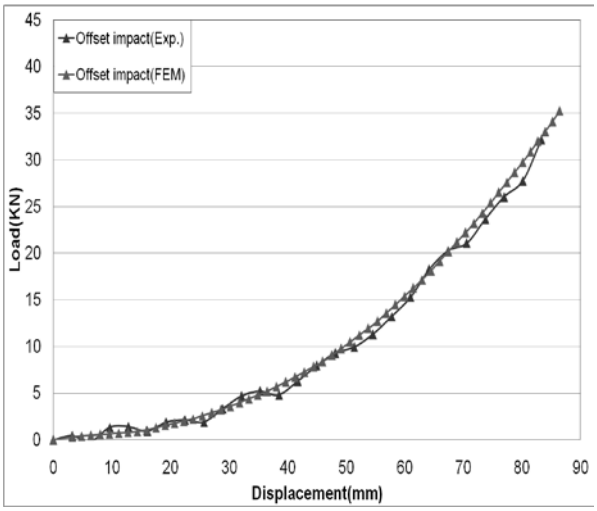

Figure 11 Comparison of experimental and predicted load-displacement curve for impact with offset angle of 15°

Table 4 Experimental fracture time and absorbed energy of CFRP guarder belt for impact with offset angle of 15°

	Experiment	F.E.M
Fracture time (msec)	5.42	5.93
Location of the fracture	T3	T3
Absorbed energy (J)	865	973

for the impact with offset angle of 15°. The fracture time and the absorbed energy are almost exactly predicted. The fracture time for the offset impact test is slightly longer than that for vertical impact, but the absorbed energy is almost same for the both case.

The experimental strain variations at three locations in the specimen compare with the numerical ones as shown in Figure 12. The strain of each locations increase with time transit nonlinearly. Both results of the strain variations at the locations of T1 and T2 agreed well.

CONCLUSIONS

The CFRP guarder belt was developed for the purpose of designing impact energy absorption member under side collision. The drop weight impact tests were carried out and the impact response behavior and the absorbed energy of the CFRP door guarder belt under impact loading were examined by using the numerical analysis and the experimental results. From these results, we could be concluded as below.

1. The CFRP guarder belt absorbed crash energy along the entire length of it and tension stress is applied on both the upper and lower side of belt.

2. From the comparison of FEM results with the experimental ones for the specimens, the proposed numerical method by ANSYS code was supposed to be useful for analyzing the CFRP guarder belt.

3. The fracture time of the CFRP guarder belt can be predicted by using FEM and fracture criteria of composite materials and agreed well with the experimental fracture time.

4. The impact response behavior and impact strength of the CFRP guarder belt were obtained by the tower drop weight impact test.

The CFRP guarder belt contributes to light-weighting and safety improvement of safety of the car body greatly is supposed.

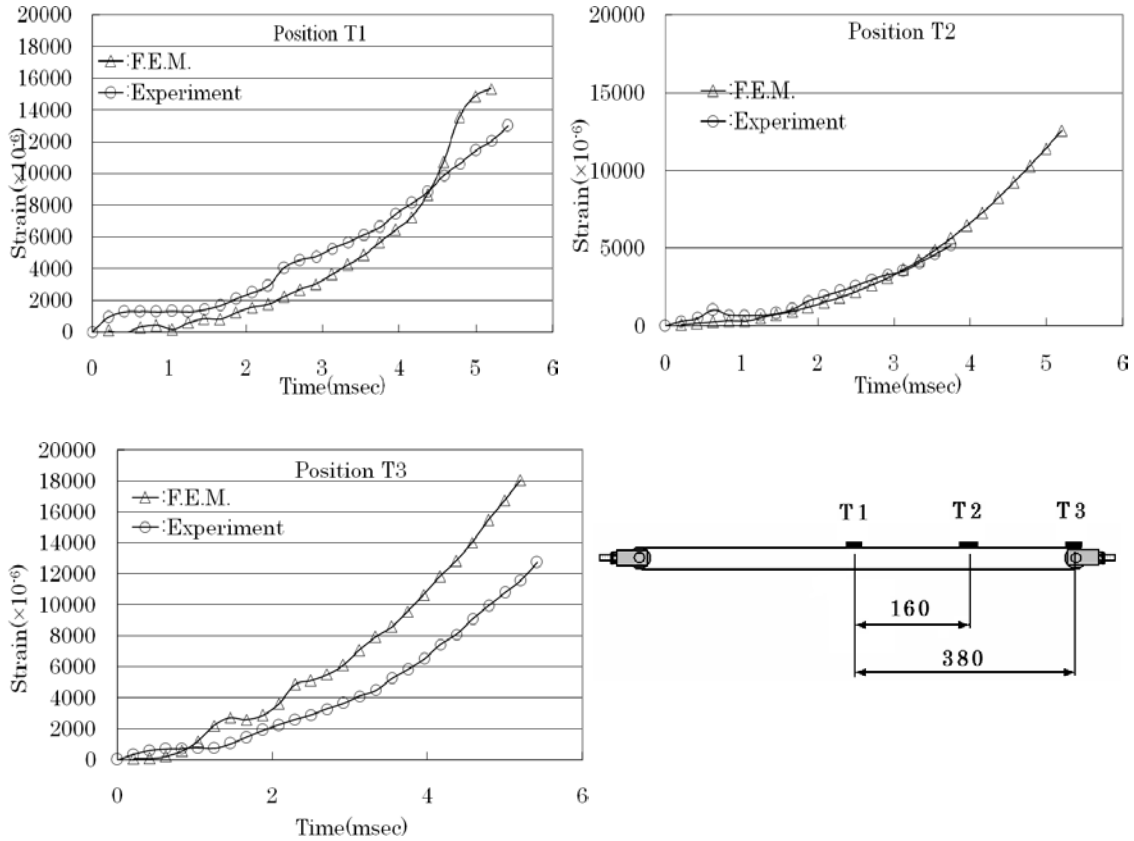

Figure 12 Comparisons of experimental and predicted the strain variation for impact with offset angle of 15°

ACKNOWLEDGEMENTS

This study was conducted as part of the Japanese National Project "R&D of Carbon Fiber-Reinforced Composite Materials to Reduce Automobile Weight" supported by NEDO (New Energy and Industrial Technology Development Organization).

The authors acknowledge the assistance of Toray Industries, Inc. who supplied the materials for these test specimens.

References

1. G. Ben, T. Uzawa, H.S. Kim, Y. Aoki et. al., J. JSME Series A, 70 (694), 824, 2004 (in Japanese)
2. Ari G. Caliskan., Proceedings of IMECE 2002, November17-22, 2002
3. H. S. Kim, G. Ben, Y. Aoki, A. Shikada., Proceedings of the 5th Japan-Korea Joint Symposium on Composite Materials, October, 2005
4. Y. Aoki and G. Ben., IATSS Review, 29(4), 21, 2005 (in Japanese)

5. G. Ben, Y. Furuta, T. Uzawa., Proceedings of the 14th Conference on the JSME Computational Mechanics Division, November, 2003 (in Japanese)

6. Yoshio Aoki, Goichi Ben, Yuka Iizuka, Key Engineering Materials, 334-335, 197, 2006

7. Yoshio Aoki, Goichi Ben, Hyoung Soo Kim, Akihisa Tabata, Proceedings of conference of the Society for the advancement of material and process engineering, L266, May, 2008

8. Hyoung Soo Kim, Goichi Ben, Yoshio Aoki, Proceedings of the US-Japan Conference on Composite Materials 2008, AUT-3, June, 2008

9. Yoshio Aoki, Goichi Ben, Hyoung Soo Kim, Proceedings of Internetional Crashworthiness Conference 2008, 2008-080, July, 2008Reference 1

Previous Paper ***Back to Programme*** ***Back to Topic*** *Next Paper*